

# Delivery of the Second Generation VLT Secondary Mirror (M2) Unit to ESO

Robin Arsenault<sup>1</sup>  
 Elise Vernet<sup>1</sup>  
 Pierre-Yves Madec<sup>1</sup>  
 Jean-Louis Lizon<sup>1</sup>  
 Philippe Duhoux<sup>1</sup>  
 Ralf Conzelmann<sup>1</sup>  
 Norbert Hubin<sup>1</sup>  
 Roberto Biasi<sup>2</sup>  
 Mario Andrighettoni<sup>2</sup>  
 Gerald Angerer<sup>2</sup>  
 Dietrich Pescoller<sup>2</sup>  
 Chris Mair<sup>2</sup>  
 Federico Picin<sup>2</sup>  
 Daniele Gallieni<sup>3</sup>  
 Paolo Lazzarini<sup>3</sup>  
 Enzo Anaclerio<sup>3</sup>  
 Marco Mantegazza<sup>3</sup>  
 Luigi Fumi<sup>4</sup>  
 Armando Riccardi<sup>4</sup>  
 Runa Briguglio<sup>4</sup>  
 Florence Poutriquet<sup>5</sup>  
 Eric Ruch<sup>5</sup>  
 André Rinchet<sup>5</sup>  
 Jean-François Carré<sup>5</sup>  
 Denis Fappani<sup>6</sup>

<sup>1</sup> ESO

<sup>2</sup> Microgate, Bolzano, Italy

<sup>3</sup> ADS International, Valmadrera, Italy

<sup>4</sup> Osservatorio Astrofisico di Arcetri, Florence, Italy

<sup>5</sup> REOSC, St-Pierre-du-Perray, France

<sup>6</sup> SESO, Aix-en-Provence, France

The deformable secondary mirror (DSM), one of the key systems of the VLT Adaptive Optics Facility (AOF), has been delivered to ESO. It has been fully qualified in standalone mode and has successfully passed the technical acceptance Europe. Recently it was installed on ASSIST, the test bench for the AOF, and will undergo optical tests, which will complete its preliminary acceptance in Europe. With its 1170 actuators and 1.1-metre thin-shell mirror, it constitutes the largest adaptive optics mirror ever produced. The DSM constitutes a fine accomplishment by European industry and is set to become the “flagship” of the AOF on Paranal.

The Adaptive Optics Facility (AOF) is intended to transform the Very Large Telescope (VLT) Unit Telescope 4 (UT4) into an adaptive telescope. This is

accomplished by replacing the conventional secondary (M2) mirror with an adaptive secondary, implementing the Four Laser Guide Star Facility (4LGSF) and installing adaptive optics (AO) modules on the various foci. Until recently, the AO modules consisted of GRAAL (Ground Layer Adaptive optics Assisted by Lasers; Paufigue et al., 2012) for HAWK-I and GALACSI (Ground Atmospheric Layer Adaptive Corrector for Spectroscopic Imaging; Stroebele et al., 2012) for the Multi-Unit Spectroscopic Explorer (MUSE), but lately the Enhanced Resolution Imager and Spectrograph (ERIS) project has been launched and ERIS will be installed on the Cassegrain focus of UT4 with an upgraded version of the SPIFFI near-infrared imaging spectrograph. With this last addition, all instruments on UT4 will thus be optimised for use with the 4LGSF and the deformable secondary mirror.

There has been major progress since the last report in *The Messenger* (Arsenault et al., 2010), as most systems have now been delivered to ESO Garching and integrated.

## The deformable secondary mirror

The DSM was delivered to Garching on 6 December 2012. This represents a major milestone for the AOF. It should be recalled that initial efforts towards the development of the DSM and thin-shell mirrors were initiated at ESO as early as 2004 in the framework of Opticon research and development efforts. This delivery initiates the start of the AOF system tests in Garching which will last for the next 18 to 24 months.

Microgate and its partner company ADS were involved early on in the project. A feasibility study was initiated in 2004 and concluded in August 2005. A single source contract was then granted to Microgate for preliminary and final design studies, which was concluded in December 2007. A few months later, the present contract was awarded for the manufacture of the DSM.

The thin-shell mirror development followed a similar time frame. Unfortunately, Opticon funded efforts were unsuccessful

and Microgate had to resort to another supplier for the manufacture of the first science shell. REOSC was awarded the contract by Microgate in August 2009 and the mirror delivery took place in January 2012. The shell has since been refurbished with magnets, coated and integrated into the DSM. Following the delivery of the first shell, ESO placed a contract with REOSC for a second, spare, thin shell.

The DSM system and its design have been presented in a number of papers: on AOF manufacture (Arsenault et al., 2010); integration and electromechanical testing (Biasi et al., 2012); stress polishing of the thin shell (Hugot et al., 2011); and in a progress report (Arsenault et al., 2012). We will focus here on the performance of the system.

## DSM high-level functionality

The DSM is contained in a complete new M2 unit that will replace the actual Dornier M2 unit of UT4. The hub structure implements the same interface as the existing one for the telescope spider and the current Laser Guide Star Facility launch telescope. The latter will be re-installed on the new M2 unit.

The M2 mirror surface is defined by the thin-shell mirror, 1120 mm in diameter and 2 mm thick, and the reference body, which defines a reference surface for the back (concave side) of the thin shell (Figure 1). Both are made of Zerodur. The reference body (manufactured by SESO, France) is a thick optical piece, lightweighted, with hole patterns to allow the passage of the 1170 voice coil actuators. These are mounted on the cold plate and apply forces on 1170 corresponding magnets glued on the back face of the thin shell. Metallic coatings on the shell back face and the front face of the reference body act as capacitive sensors used to measure the gap between both.

In non-adaptive optics mode, a constant command is applied to the 1170 actuators to give to the thin shell the VLT M2 prescription figure. This figure will have been calibrated on the ASSIST test bench. The command is applied at a sampling rate of 80 kHz, the internal



Figure 1. The deformable secondary mirror in its test stand. In operation the thin-shell mirror is held by the actuators with a gap of  $65\ \mu\text{m}$  between the shell back face and the reference body front face. The black metallic structure surrounding the mirror is called the "EMC skirt" and shields the system from electromagnetic interference.

control loop frequency, but kept constant. The result for the telescope user is an equivalent pseudo-rigid M2 mirror like the current Dornier mirror.

The M2 local control unit (LCU) software (and the whole system) have been developed with the intention of minimising changes in non-adaptive optics mode, so that for users and telescope operators, the mirror is set up like a Dornier M2 unit. The same adjustment possibilities are

offered: two focal stations — Cassegrain and Nasmyth, focusing and centering (i.e., rotation of the mirror around its centre of curvature). The required motions are performed with a hexapod, but this is transparent to the user. The active optics of the VLT functions in exactly the same way as with the Dornier M2.

The full potential of the DSM is unleashed in adaptive optics mode: here the 1170 actuators are used to change the shape

of the mirror in order to correct the atmospheric turbulence. A  $\pm 1\ \text{N}$  force can be applied to each actuator, which provides considerable stroke for the low order modes (tip, focus and astigmatism) while much more force is required for the high order modes, which can be very stiff. The shell is operated at a gap of  $\sim 65\ \mu\text{m}$ ; given the constraint that this gap should not be below  $\sim 30\ \mu\text{m}$ , to ensure proper capacitive readout, this means that some  $\pm 30\text{--}40\ \mu\text{m}$  stroke is available for turbulence correction (for reference, a typical piezoelectric stack deformable mirror provides less than  $10\ \mu\text{m}$  total stroke). The internal control loop of the DSM operates with a given set of force/gap for each actuator. This set of gaps is updated by the adaptive optics real-time computers of GRAAL and GALACSI, and in the future, ERIS, using the Standard Platform for Adaptive optics Real Time Applications (SPARTA) architecture. The difference from a piezoelectric stack mirror, for instance, is that the DSM internal control loop manages the dynamics of the mirror in an optimal fashion. At the next iteration the SPARTA real-time computer can send a new command knowing that the previous one has been executed without time delay, creep or hysteresis.

The SPARTA real-time computers implement various control schemes depending on the instrument that is being fed: ground layer AO correction (GLAO); laser tomography AO correction (LTAO), both with laser guide stars; and classical on-axis natural guide star AO correction (NGAO). The set of modes to be controlled can also be optimised to zonal control

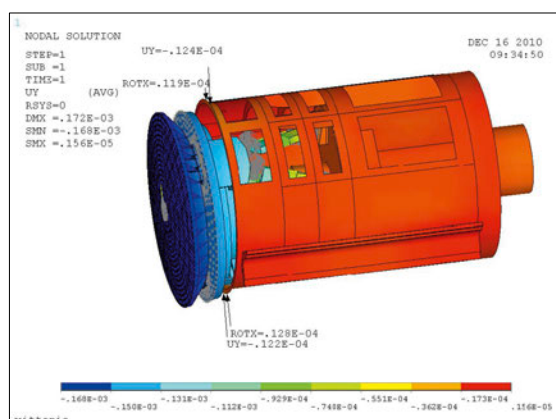
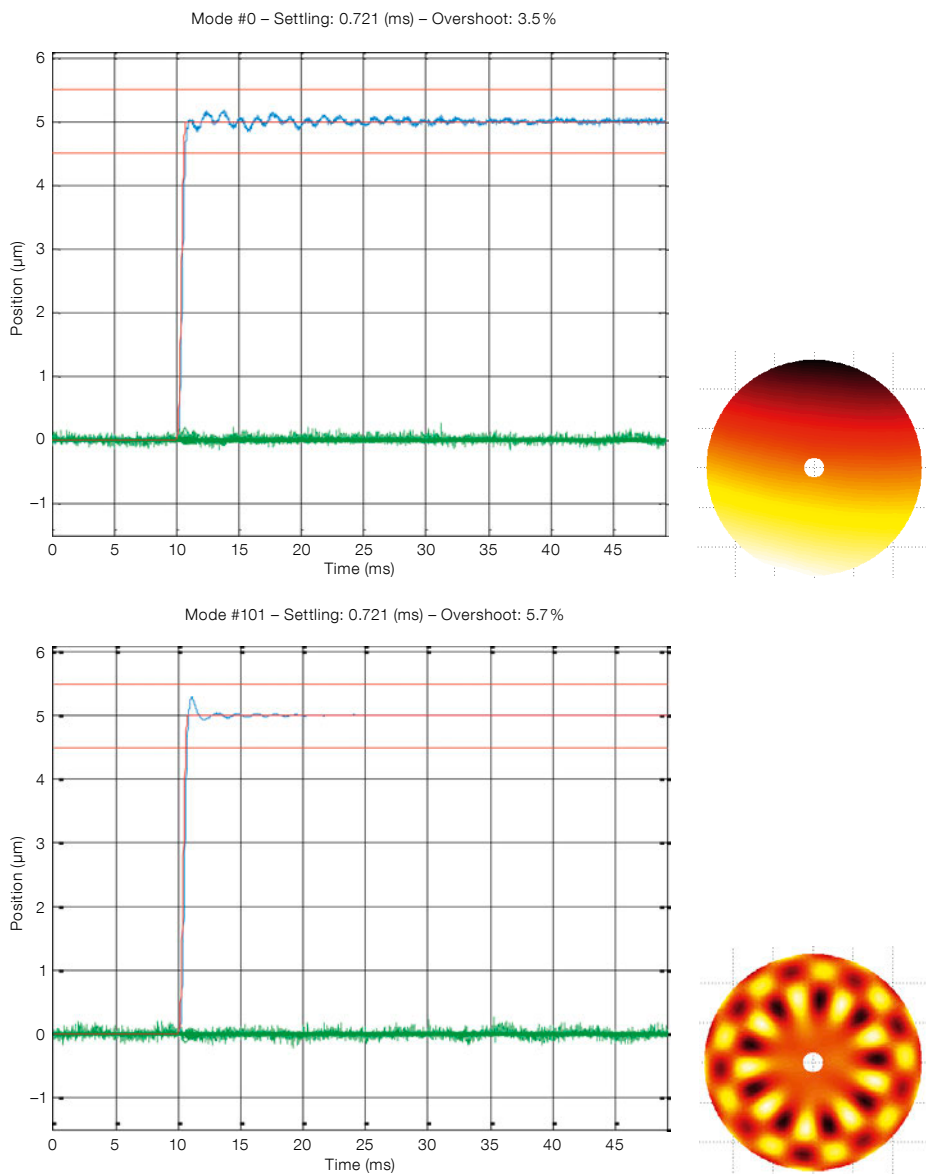


Figure 2. Finite element modelling of the complete DSM shown on the left. It is used as a baseline to compare with the experimental results. On the right, the hub with dummy weights and external encoders to measure flexure. The hub integration and service stand allows the inclination of the hub to be varied to characterise the flexure at the level of the reference body for different orientations. The results of the flexure campaign confirmed the system rigidity at  $150\ \text{N/mm}$ .



**Figure 3.** Response time performance for tilt (upper) and the natural eigenvector mode 101 (lower). The control parameters have been adjusted so that all modes have similar dynamical properties. The specification was 1.2 milliseconds at 90% of command and less than 10% overshoot; all modes are below 0.7 milliseconds. The stiffer the mode (i.e. mode 101), the higher its resonance frequency; thus the bigger challenge is for the low order modes such as tilt, focus, astigmatism, etc.

### DSM unit system tests

Testing of the DSM started a while ago at subsystem level. The Integration Progress Review was held in May 2011 and one complete week was spent at ADS and Microgate to inspect all the hardware produced by this time, before the integration of the whole DSM system. The aim was to ensure that all components were validated before this final step. Both contractors developed custom tools and test setups for this phase of the project.

At Microgate, where the electronics and software were developed, the corresponding subsystems were inspected and tested: electronic control boards, actuators, racks and software. A massive amount of data was acquired, which has been reviewed by ESO, and will be built into the system as internal calibration data used during system operation. Mechanical subsystems were also tested and inspected at the ADS premises. The hexapod motion characteristics were tested: centering, focusing, change of focal station (Nasmyth to Cassegrain), full range, positioning accuracy and motion cross-coupling. Particular care was taken to assess the mechanical rigidity of the system (see Figure 2).

(individual actuators), stiffness modes (natural modes of the DSM) or Karhunen–Loeve, or any set defined by the AO specialist. Furthermore, an online algorithm monitors the interaction matrix during the observation in order to identify mis-registration between the DSM and the wavefront sensors and to update the command matrix to optimise the correction.

A subtle consequence of using an adaptive secondary is that the active optics of the VLT will be inoperative. The active

optics Shack–Hartmann sensor is blind to the telescope aberrations since it is fed after the DSM and thus sees a perfectly corrected wavefront. In other words, the telescope internal aberrations and misalignments are corrected by the DSM. The strategy is thus to offload the quasi-static aberration seen on the DSM directly to the M1 mirror actuators. Note that the coma correction that is done by the centering correction of the M2 unit is the same, whether in non-adaptive or adaptive optics mode.

### Performance

The most impressive results of the whole system test campaign are probably the critical performance specifications, which have all been met. Among these are: the residual wavefront error after adaptive optics correction, the response time (see Figure 3), the chopping stroke and its response time. The main verification of the DSM performance is the follow-up error test. Numerical phase screens have

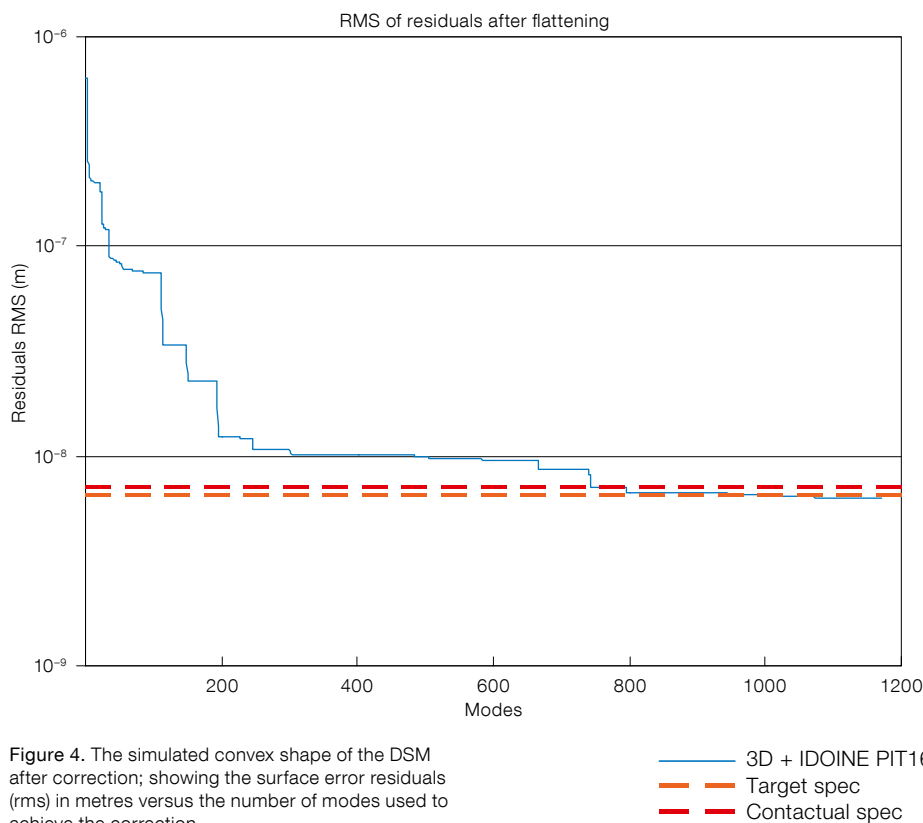


Figure 4. The simulated convex shape of the DSM after correction; showing the surface error residuals (rms) in metres versus the number of modes used to achieve the correction.

been simulated at ESO for a calibrated condition of 1.5 arcseconds at a wavelength of 0.5  $\mu\text{m}$ , 20 degrees elevation angle and 1000-mode correction. These are quite demanding conditions. From these phase screens one can easily infer the shape that must be taken by the DSM to correct the wavefront. A file containing the time history for all actuators has been provided to Microgate.

The test then proceeds by switching on the DSM and fooling it into believing that the capacitive sensors measure the distances in the time history file. The internal control loop then corrects these offsets. The system measures the capacitive sensor signals versus time and makes a few simple assumptions about time delay. At each calculation cycle, a delta can be measured between the real mirror position and the sent perturbation. This constitutes the main part of the error signal. If the error due to the high order modes not corrected by the DSM is added to this delta, then the result gives the performance of the system in terms of resid-

ual root mean square (rms) wavefront error. The result of this test gives 131.5 nm rms wavefront error while the specification requests 149 nm rms. The internal control loop of the DSM (between coils and capacitive sensors) represents a huge asset at the time of testing as it allows the subsystem to be fully qualified before it is integrated into the AOF with guide stars, external real-time computer and optical Shack–Hartman sensors.

#### Thin-shell mirror

The convex face of the thin shell is polished to the nominal M2 optical prescription and then the optical piece is thinned to the 2 mm nominal thickness. The defects in the convex shape can be relatively high (several micrometres) if they represent low order deformations; but these can then easily be corrected by the actuators of the DSM. A computer program has been developed by the Osservatorio Astrofisico di Arcetri in order to assess the forces required to obtain

the M2 nominal prescription figure from the actual convex shape. The specification to be fulfilled by the optical supplier is then to provide a convex face that requires less than 0.1 N (10% of full range) to bring the shell to the 8 nm rms surface error.

The first science shell reached the specified quality requirement: the convex shape could be brought to 8 nm rms surface error by correcting  $\sim 800$  modes and this required  $\sim 0.1$  N force (see Figure 4). If all the 1170 modes are corrected, the surface error is reduced further, but higher forces are required.

The next challenge was the thinning and accurate surfacing of the back face of the thin shell. In order to ensure good dynamical behaviour (response time, electronic damping and homogeneous and low-noise capacitive sensor readout), the gap between the reference body and thin shell must be homogeneous. The criteria is thus to thin the shell to a homogeneous thickness. Here there is both a constraint from the polishing and also from the measurement: the acoustic devices used to measure the thickness, although they possess sufficient accuracy, are somewhat sensitive and measurements can easily be degraded by conditions (surface cleanliness, sensor/surface interface, surface roughness, parasitic devices running simultaneously, etc.).

Despite these difficulties the first shell was realised to specification and delivered to ADS in January 2012. Following this, an aluminium coating was applied to the back face, leaving 1170 circular apertures for the gluing of the magnets (Figure 5). This coating has essentially an electrical purpose. After the gluing of all the magnets, the optical coating is deposited on the convex side.

The last integration step is to glue the central membrane onto the shell; this is done in the setup with the shell held up by the actuators and kept in position for several hours while the glue is curing. Note that the membrane allows tip and tilt and piston motion (along the optical axis) of the shell, while restraining motion perpendicular to the optical axis.

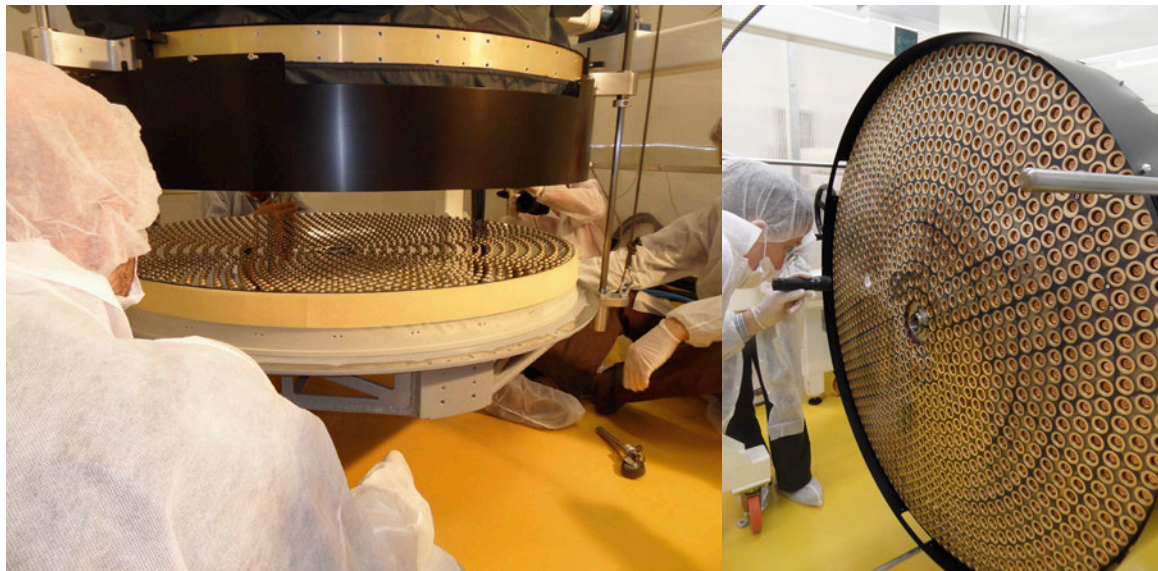


Figure 5. Left: The thin shell being dismantled. The magnets glued to the back face are visible. Right: The front face of the reference body. The 1170 recesses for the magnets surrounded by the chemically deposited rings of silver coating (for capacitive sensing) can be clearly seen. The copper parts inside the reference body recesses are the caps on top of the voice coil actuators.

ESO has awarded a contract to REOSC for a second science shell that will be used as a spare. The latter will be fully characterised before the DSM is shipped to Chile for commissioning.

#### Handling and maintenance

A fear often expressed in dealing with such a fragile thin-shell mirror is the danger of hosting it in a VLT system. The concern is certainly justified, but the suppliers have taken particular care in developing detailed procedures and a set of handling tools to ensure that any handling will be conducted under the best

and safest conditions. For instance, a multi-purpose container has been developed for the thin shell. Its design is the result of years of experience with previous deformable thin-shell mirrors and detailed finite element modelling (FEM). The concept consists of two halves holding the thin shell in a sandwich and the spacers between these two halves are calibrated to exert a pre-defined load on the shell.

The shell transport box (STB; Figure 6, left) fulfils several functions as well as transport of the shell: the lower (concave) half is used as receptacle for the shell removal and installation on the DSM; the complete STB with shell can be sus-

ended from a reverse “U” shape handling device allowing the shell to be flipped; and the convex half of the shell can be used as a “coating body”.

A similar philosophy has been applied to the DSM system itself. Other tools enable various maintenance operations: a test stand has been provided for the hub alone or with the DSM; another stand has been provided for the DSM assembly alone (Figure 6, right); a stand hosts the hexapod when it is removed from the hub; and dummy weights are provided to replace missing components, allowing continual use of the same tools in a balanced configuration.

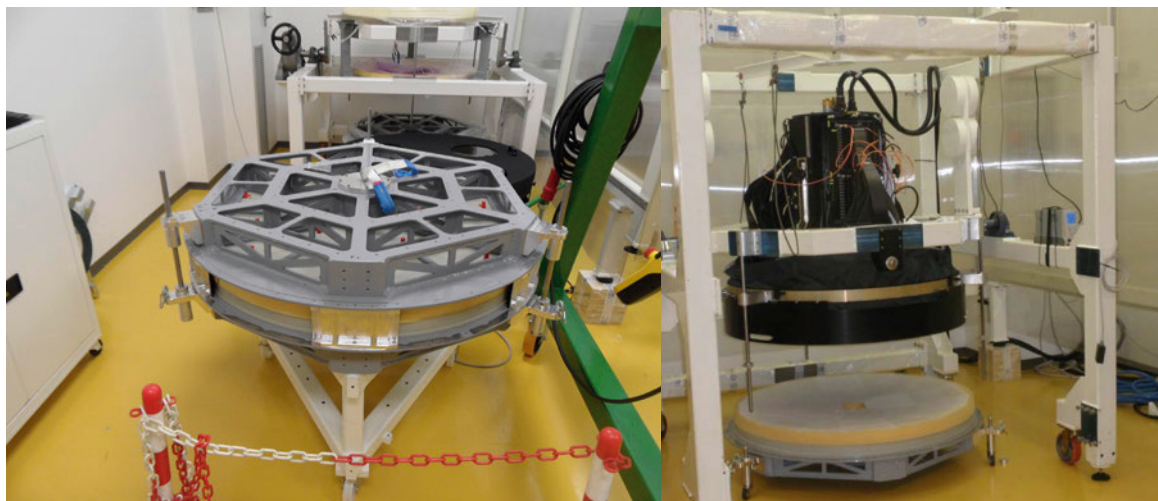


Figure 6. Left: the shell transport box, which is the DSM multi-purpose handling and protection equipment, is shown. Right: the DSM test stand allows the DSM, with its electronics, to be fully operational in the laboratory.

## Next phases and key milestones for the AOF

Now that the DSM has been successfully delivered, the subsequent sequence of events is straightforward. The AOF project has now reached a stage where most of the tasks are now sequential and on the critical path. In January 2013 the DSM was mounted on ASSIST (Stuik et al., 2012). There a team from Arcetri Observatory and ESO will fully characterise the DSM optically. This phase will last around four months and is still the responsibility of the contractor.

ASSIST, with its 1.7-metre main mirror provides a complete optical setup for the DSM; no simple task for a convex secondary mirror (Figure 7). With the use of a fast interferometer, the DSM will first be characterised optically. For the other tests with GRAAL and GALACSI, the input module of ASSIST simulates a constellation of sources, natural and laser guide stars defocused and aberrated by calibrated turbulence. The AO modules can be mounted on ASSIST and an output optical module simulates the optical and mechanical interface of the VLT Nasmyth focus.

During that time GRAAL will complete its standalone tests and validation. Then, mounted on ASSIST with the DSM, the whole assembly will be used to fully qualify the adaptive optics loop. The source module of ASSIST with phase screens to generate calibrated turbulence will feed the DSM and GRAAL. The GRAAL real-time computer and wavefront sensor will create realistic conditions for closed-loop operation. The natural guide star mode on-axis of GRAAL will first be tested.

These tests will constitute a strong basis to continue with GRAAL GLAO correction mode tests and characterisation. Then GRAAL will be replaced by GALACSI and the GLAO correction mode of GALACSI tested. The second mode of correction of GALACSI (LTAOs for the MUSE narrow-field mode) will then follow. Before shipment the DSM will be refurbished with the spare thin shell whose delivery is planned for the end of 2013. The second shell in the DSM will then be fully qualified and validated on ASSIST.

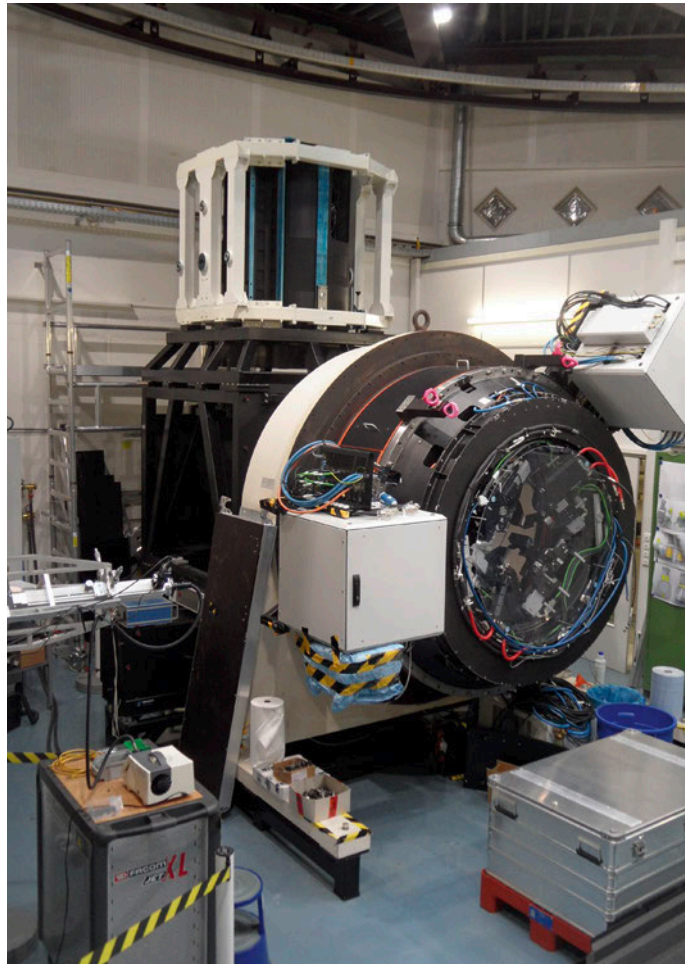


Figure 7. The DSM mounted on the ASSIST test bench in the ESO Garching integration laboratory at the start of the test phase. GRAAL is in the foreground.

The initial commissioning activities of the AOF are expected to last through 2015.

### Acknowledgements

Many thanks are due to numerous people who have been involved, occasionally, but over a period of many years, and provided unfailing support to the project: F. Koch for structure analysis and counselling; M. Cayrel for supporting critical steps of development of the thin shell; S. Stanghellini for his expert advice and enthusiasm during the reviews and latest acceptance procedures; J. Schimpelsberger for his diligence with all contract amendments and negotiations; M. Duchateau and R. Brast for their help with electronics design/acceptance reviews. C. Dupuy and S. Tordo have always been active in the background to help with integration and interfaces and R. Stuik from the University of Leiden has been leading the development of ASSIST and helping with the interfacing of the DSM on the test bench. Finally, our Paranal colleagues P. Sansgasset and G. Hüdepohl, who have been our “base of knowledge” concerning VLT M2 units, are thanked together with J.-F. Pirard for preparing the arrival of the AOF in Paranal and the DSM in particular.

### References

- Arsenault, R. et al. 2010, *The Messenger*, 142, 12
- Arsenault, R. et al. 2010, *Proc. SPIE*, 7736, 20
- Arsenault, R. et al. 2012, *Proc. SPIE*, 8447, 0J
- Biasi, R. et al. 2012, *Proc. SPIE*, 8447, 88
- Hugot, E. et al. 2011, *A&A*, 527, A4
- Kuntschner, H. et al. 2012, *Proc. SPIE*, 8448, 07
- Paufique, J. et al. 2012, *Proc. SPIE*, 8447, 116
- Stroeble, S. et al. 2012, *Proc. SPIE*, 8447, 115
- Stuik, R. et al. 2012, *Proc. SPIE*, 8447, 118